JOURNAL OF SPACECRAFT AND ROCKETS
Vol. 35, No. 4, July–August 1998

Application of Numerical Multizone Approach to the Study of Satellite Thruster Plumes

D. Giordano*
European Space Agency, 2200 AG Noordwijk, The Netherlands
M. Ivanov,† A. Kashkovsky,‡ and G. Markelov‡
Institute of Theoretical and Applied Mechanics, Novosibirsk 630090, Russia
G. Tumino§
European Space Agency, 2200 AG Noordwijk, The Netherlands
and
G. Koppenwallner¶
Hyperschall Technologie Göttingen, 37191 Lindau, Germany

The work performed during the implementation phase of an integrated set of computer codes developed to study plume flows generated from satellite main engines and thrusters is described. The major aim of the work was to achieve the capability to cover the complete cycle of gasdynamics analyses required to assess the impact that plume impingement effects may have on the satellite and on its sensitive payload or instrumentation. A simplified configuration of the European Space Agency's satellite for the X-Ray Multi-Mirror Mission was considered as a test case for the purpose of implementing and testing the computer codes. In this regard, the issue of major concern consisted of the estimation of the thrust loss produced by plume impingement during the injection maneuver of the satellite into a higher perigee orbit. Results obtained by Navier–Stokes, direct simulation Monte Carlo, and test particle Monte Carlo calculations are described, and the flow patterns settling in during thruster firing in the regions of interest are discussed. The major finding of the study was the detection of a serious incompatibility between the preliminary assumed design orientation of the satellite thrusters and the flight dynamics requirements imposed by the satellite mission. In conclusion, the study fully provides evidence of the critical role and usefulness of this kind of numerical analyses in providing answers contributing to the optimization of successful satellite design.

Nomenclature

A	= axial force per unit area, N/m^2
$\bar{A}$	= species contributions to A, N/m^2/kg
B	= breakdown parameter
F	= nozzle thrust, N
Ma	= Mach number
$\dot{m}$	= mass flow rate, kg/s
P	= pressure, N/m^2
R	= equivalent gas constant, J/kg/K
T	= temperature, K
X, Y	= nozzle axial and radial coordinates, m
x, y, z	= satellite body axis coordinates, m
Z_r	= rotational-relaxation collision number
γ	= equivalent specific-heat ratio
ρ	= mass density, kg/m^3
ϕ	= circumferential angle, deg

Subscripts

c	= chamber conditions
calc	= calculated value
nom	= design nominal value

Presented as Paper 97-2538 at the AIAA 32nd Thermophysics Conference, Atlanta, GA, June 23–25, 1997; received June 25, 1997; revision received March 9, 1998; accepted for publication March 16, 1998.

*Research Engineer, Aerothermodynamics Section, European Space Research and Technology Center, P.O. Box 299. Member AIAA.
†Head, Computational Aerodynamics Laboratory, 4/1 Institutskaya st. Member AIAA.
‡Research Scientist, Computational Aerodynamics Laboratory, 4/1 Institutskaya st.
§Research Engineer, Chemical Propulsion Section, European Space Research and Technology Center, P.O. Box 299.
¶Senior Research Engineer, Max Planck Strasse 1.

Introduction

PLUME flows produced during satellite operations generate unavoidable effects, namely, contamination of surfaces, production of local atmospheres, severe heating, thrust losses, and perturbing forces and moments on the satellite and on its payload and instrumentation. The sensitivity of payload and instrumentation, as well as the overall satellite performance, requires the prediction of the effects mentioned and establishes the accuracy according to which they must be predicted and dealt with for successful design. A typical cycle of gasdynamics analyses for quantitative prediction of plume effects starts from the nominal operating conditions of the satellite main engines or thrusters; includes the simulation of the continuum flow in an expansion nozzle, of the transitional flow in the plume near field, and of the free-molecular flow in the plume far field (if necessary); and ends with the assessment of aerodynamic forces and moments, mass fluxes, and heat transfer on the spacecraft structure. Note that the plume impingement might cause a decrease in the local Knudsen number in the vicinity of the spacecraft surfaces; in this case, it becomes necessary to consider the presence of transitional flows embedded in the free-molecular field. In our methodology, the nozzle flow is calculated by the Navier–Stokes solver ROGER, which is the perfect-gas adaptation of the second-order accurate, point and line implicit, time-marching Navier–Stokes solver TINA[1] (Thermochemical Implicit Non-Equilibrium Algorithm), which finds primary application for viscous flows in thermochemical nonequilibrium. The main purpose of the Navier–Stokes code is to produce the radial profiles of the flow parameters, namely, temperature, density, composition, and velocity vectors, required by the direct simulation Monte Carlo (DSMC) two- and three-dimensional parallel code SMILE[2] (Statistical Modeling in Low-Density Environment). The DSMC code simulates the plume near field, i.e., the field that extends from the nozzle exit to the free-molecular region. In this work, the interface between Navier–Stokes and DSMC calculations was made coincident with the nozzle exit section. A Maxwellian distribution function based on the flow parameters from the Navier–Stokes solution was

used for the DSMC inflow. The assumption of equilibrium flow conditions for the DSMC inflow introduces no considerable distortion into the plume near field. This was demonstrated in subsequent applications[3–5] of our methodology, where we have also learned that the Navier–Stokes calculation does not need to be terminated at the nozzle exit section but can be extended to an inner core of the plume near field, where the flow can still be considered sufficiently continuous. Alternatively, the DSMC calculation can be started inside the nozzle at a location somewhere upstream of the exit section, if the exit Knudsen number is high enough to warrant the use of DSMC. The extent of agreement between the two calculation methods in the overlapping region has been found to be quite satisfactory and constitutes a measure of the quality and accuracy of the simulation. The DSMC solver employs a majorant-frequency scheme with coupling free-cell and cell algorithms.[6] Intermolecular collisions and energy exchanges between translational and rotational molecular degrees of freedom are described according to the variable-soft-sphere and the Larsen–Borgnakke models,[7] respectively. The latter model uses a constant rotational-relaxation collision number Z_r. The plume near field usually requires a two-dimensional axisymmetric calculation, and therefore the DSMC method is applied in the corresponding formulation, although, depending on the nozzle location relative to other spacecraft surfaces, a three-dimensional analysis may become necessary. According to the particular satellite configuration, the analysis is continued in the outer regions of markedly free-molecular flow (far field) by a third code based on the test particle Monte Carlo (TPMC) method. The input conditions for the free-molecular calculation are provided by the DSMC solution on the boundary of the near-field computational domain. The coupling between the DSMC and TPMC domains is performed using an ellipsoidal distribution function that allows one to take into account the nonequilibrium condition of the flow with substantially different parallel and perpendicular temperatures.[8] The use of the TPMC method to calculate the plume far field and its interaction with the spacecraft surfaces is an important feature of our multizone approach. From a computational point of view, the TPMC method is more efficient than the collisionless DSMC method. Moreover, contrary to engineering methods in use to simulate plume far fields,[9] the method takes into account multiple molecular reflections during the plume–surface interactions, and in addition to the flow parameter distributions on the satellite surfaces, our implementation of the TPMC method provides the flow parameters in the space region around the satellite. The latter parameters are obtained from the knowledge of the residence times spent in the grid cells by the particles during their tracing. The final goal of the rarefied gasdynamics simulations (DSMC and/or TPMC) is the determination of the mass flux distribution and the (local and integrated) thermal and dynamical loads that the cloud of exhaust gases imposes on the satellite structure. More specific details about theoretical aspects, physical models, and numerical techniques implementented in the DSMC and TPMC codes can be found in Refs. 2, 6, and 10–13.

The described methodology has been successfully applied to resolve satellite design problems associated with plume flows.[3,4] The following sections describe the application to the thrust-loss problem encountered during the development phase of the European Space Agency's satellite for the X-Ray Multi-Mirror Mission (XMM). The thrust loss originates from the plume impingement on the satellite conical body produced by the firing of four (of the eight) hydrazine thrusters, situated on the satellite base. These firings occur during the injection maneuver into a higher perigee orbit, and the thrust loss could seriously affect the fuel budget or impair the maneuver if the loss exceeds 5% of the foreseen nominal thrust (80 N).

XMM Satellite Application

Flow in the Thruster Nozzle

The axisymmetric nozzle flow, generated from the decomposition of hydrazine in the thruster chamber, was assumed chemically frozen and calculated with the Navier–Stokes solver ROGER. The calculation assumed an adiabatic nozzle wall and was carried out for the assigned operating chamber conditions (Table 1) and mixture composition (Table 2) from the nozzle inlet to the nozzle exit section, where a first-order extrapolation of the relevant flow variables was imposed as a boundary condition. The gas constants R and γ (Table 3) have been evaluated, respectively, from the assigned composition of Table 2 and from arguments of consistency with measured performance characteristics of the thruster.[14] Particular care was devoted to the accuracy of the nozzle flow simulation because it provides the nozzle exit conditions required by the DSMC code. The primary aspect investigated was the grid independence of the solution. The initial grid had a resolution of 150×50 points along the axial and radial directions, respectively. The grid independence was checked first by doubling the number of points in the axial direction. As illustrated in Fig. 1 for the isobars, the isolines corresponding to the different grids are, generally, in satisfactory agreement; however, they show a manifest nonvertical slope near the nozzle axis, a clear sign of insufficient resolution along the radial direction. For this reason, the corresponding number of points was doubled and even quadrupled to achieve a satisfactory grid independence and solution convergence (Fig. 2). The latter was confirmed (Fig. 3) by the solution obtained from the Navier–Stokes solver BLT,[15] based on an unfactored implicit upwind-differencing finite volume scheme, on a completely different grid. A final check of the solution accuracy was provided by the rather flat axial profile of the mass flow rate

Table 1 Thruster operating chamber conditions

P_c, N/m^2	T_c, K	ρ_c, kg/m^3
9.7×10^5	1473.15	1.03

Table 2 Mixture composition (molar fractions) at exit of thruster chamber

NH_3	N_2	H_2
0.216	0.298	0.486

Table 3 Gas constants

R, J/kg/K	γ
639.26	1.38

Table 4 Nominal and computed performance characteristics of the thruster (see also Fig. 4)

Type	Grid	$\dot{m}$, g/s	F, N
Nominal	——	8.84	20.00
Computed	150×100	8.89	20.76
Computed	150×200	8.80	20.67

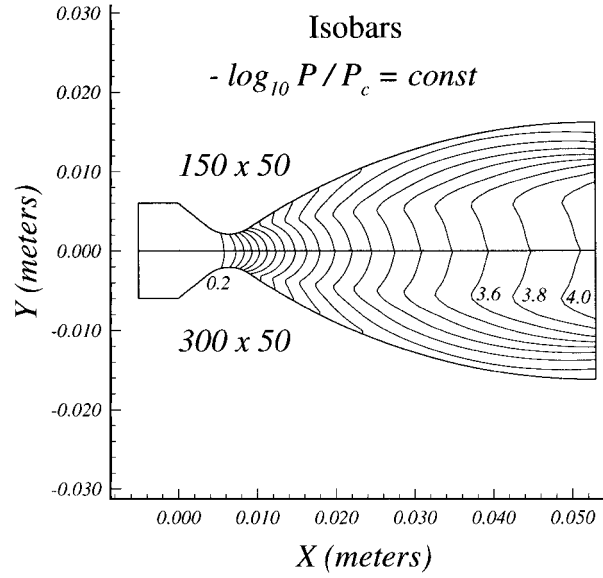

Fig. 1 Grid independence in the axial direction.

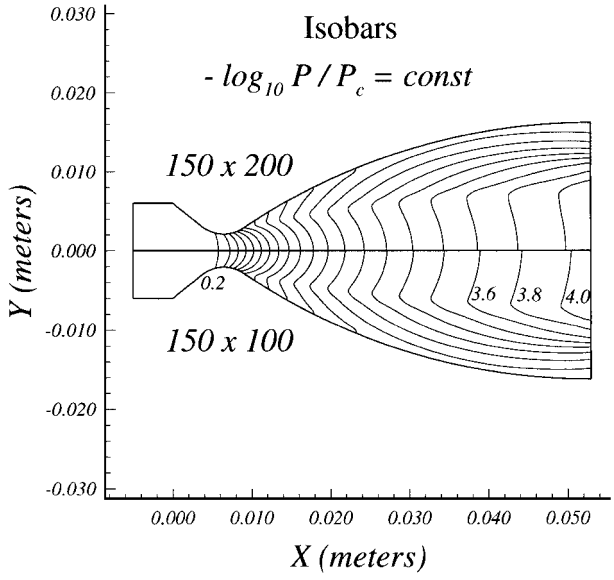

Fig. 2 Grid independence in the radial direction.

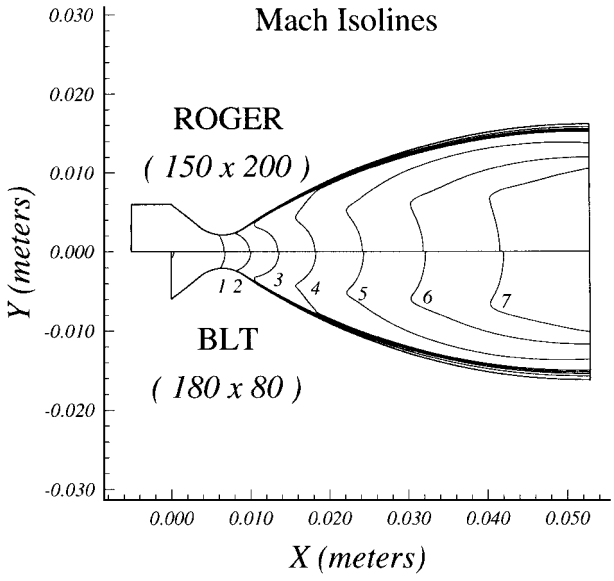

Fig. 3 Comparison between solutions from different Navier–Stokes codes.

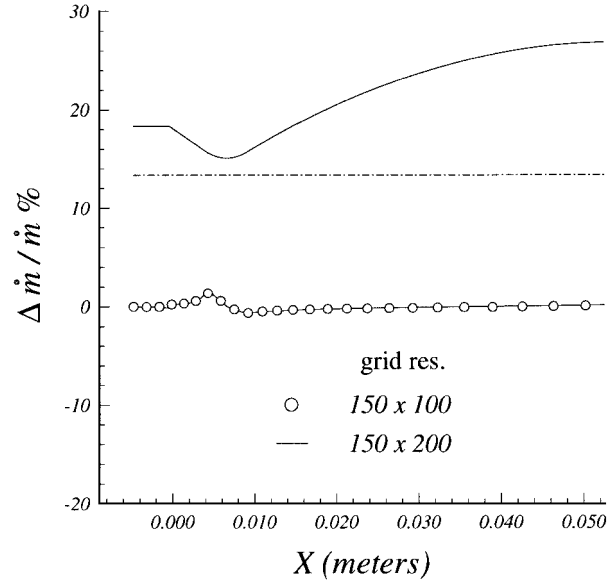

Fig. 4 Axial profile of the mass flow rate error.

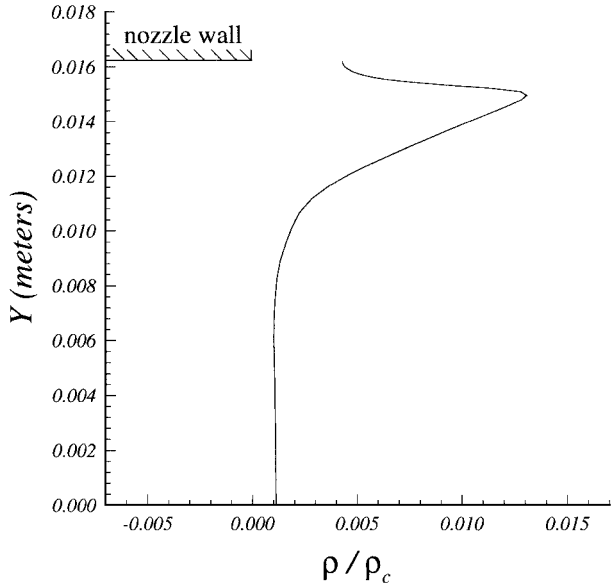

Fig. 5 Density profile at the nozzle exit section.

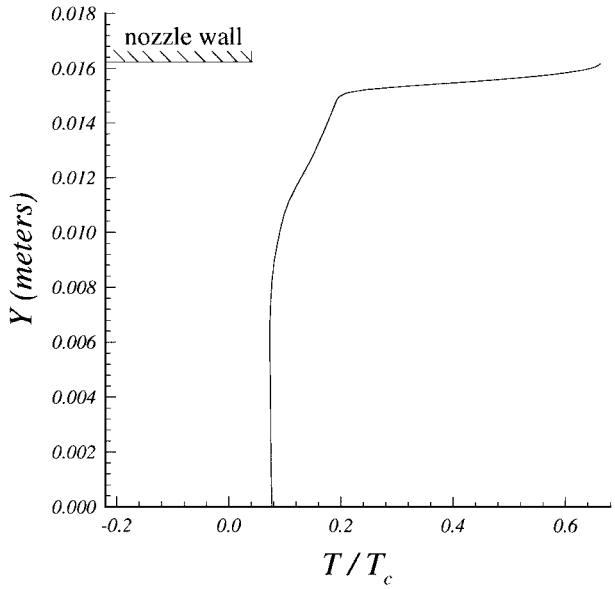

Fig. 6 Temperature profile at the nozzle exit section.

error (Fig. 4) and the good agreement (Table 4) between nominal and calculated mass flow rate and thrust. The error shown in Fig. 4 is defined as $100 \times (\dot{m}_{\text{calc}} - \dot{m}_{\text{nom}})/\dot{m}_{\text{nom}}$, with $\dot{m}_{\text{nom}} = 8.84$ g/s. The error peak upstream of the throat is a numerical effect due to a grid resolution not sufficiently suitable for the elliptic character of the flow; however, the error is less than 2% and can be considered acceptable for the purpose of the present study.

The isobar pattern of Fig. 2 reveals the typical expansion in a contoured nozzle with the presence of a compression wave originated from the sudden change in the curvature of the divergent part. The pressure drop of slightly more than four orders of magnitude accelerates the gas mixture to leave the nozzle exit with Mach number $Ma \simeq 8$ (see Fig. 3). The exit profiles of temperature, density, and velocity vectors are shown in Figs. 5–7; together with the mixture composition given in Table 2, they represent the input information for the DSMC simulation of the plume near field.

Plume Near and Far Field

The DSMC simulation began with a calculation of the plume in a rectangular region adjacent to the nozzle exit to capture the main characteristics of the flow structure and to achieve a good resolution of the flow gradients in the still dense core of the plume (Fig. 8; the DSMC computational domain is the upper rectangular region

where the isolines are drawn; the lower-half flowfield, including the nozzle, is a mirrored image of the upper-half one). This region covers essentially the initial expansion of the plume, where the latter is still influenced by the Mach lines emanating from the inside of the nozzle. Vacuum conditions were assumed in the DSMC calculation as downstream boundary conditions for the expansion of the three-species nonreacting gas mixture. The choice of the upstream boundary conditions for the DSMC calculation at the nozzle exit section was primarily dictated by the need for a simple matching between the different characters of the computational grids used in the Navier–Stokes (body-fitted and structured) and DSMC (unstructured and Cartesian) domains. This choice certainly induces some errors in the subsonic flow of the boundary layer near the nozzle lip; however, such errors affect only the flow that originates in the nozzle boundary layer and expands into high angles from the nozzle centerline. The mass rate of the flow deflected at high angles is less than 1% of the total flow rate, and therefore it does not affect appreciably forces and moments on the satellite due to plume impingement. The background grid in the DSMC computational domain consisted of $160 \times 50 = 8000$ cells. When the steady-state, converged solution was achieved, the grid adaptation based on the local mean free path had generated approximately 31,000 collisional cells with the presence of almost 340,000 model particles. Figure 8 shows how the isobars of Fig. 2 (upper-half flowfield) evolve in the DSMC computational domain. The two representative streamlines denote the presence of a core of geometrically conical flow surrounded by a peripheral layer in which the flow is compelled to adjust to the nozzle contour. The enveloping action of the peripheral layer evolves into the formation of a shock wave that converges downstream of the exit section, approximately at 60% of the thruster length, and reflects to form a rather conically shaped secondary shock wave. The breakdown parameter[7] map (Fig. 9) shows a substantially continuum flow ($B \leq 0.05$) in most of the rectangular computational domain. Rarefaction effects are evident in the vicinity of the nozzle lip and in the interior of the shock wave coming from the nozzle. Notwithstanding the continuum nature of the flow, the rarefaction in the reflected shock wave is also visible. The DSMC computational domain was then enlarged (upper rectangular region of Fig. 10, where the isolines are drawn), and the simulation was continued from the boundary of the previous domain. At this boundary, the flow parameters defining an ellipsoidal distribution function were computed from the inner domain DSMC solution. The resulting distribution function was then used to model the particles entering the enlarged domain, where the grid had larger cells, namely, $125 \times 60 = 7500$ background cells with 86,000 collisional cells after final adaption and 320,000 model particles at steady state. The intent of the calculation in the enlarged domain was to meet the requirement of obtaining an acceptable situation of collisionless flow ($B > 1$) on its boundary to allow the subsequent free-molecular analysis around the complete configuration of the satellite. The map of the isobars in the complete near field is shown in Fig. 10.

The outer boundary of the enlarged DSMC computational region was rotated 360 deg around the thruster symmetry axis to generate a cylindrical surface on which all of the flow parameters of the plume are known. Two thrusters and their corresponding cylindrical

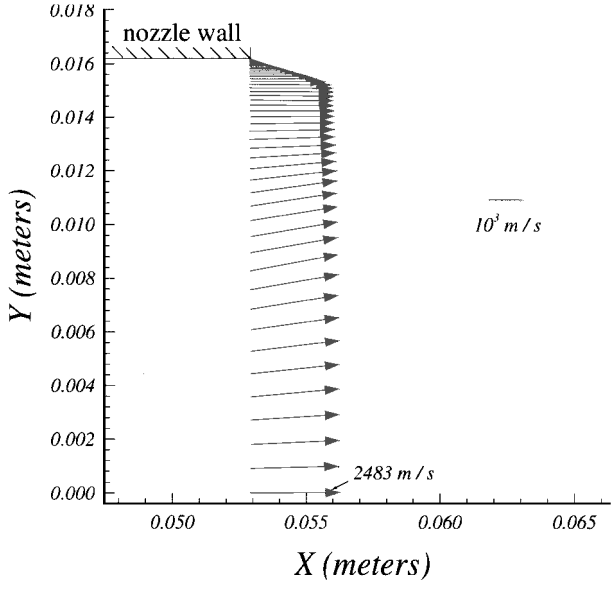

Fig. 7 Velocity vector profile at the nozzle exit section.

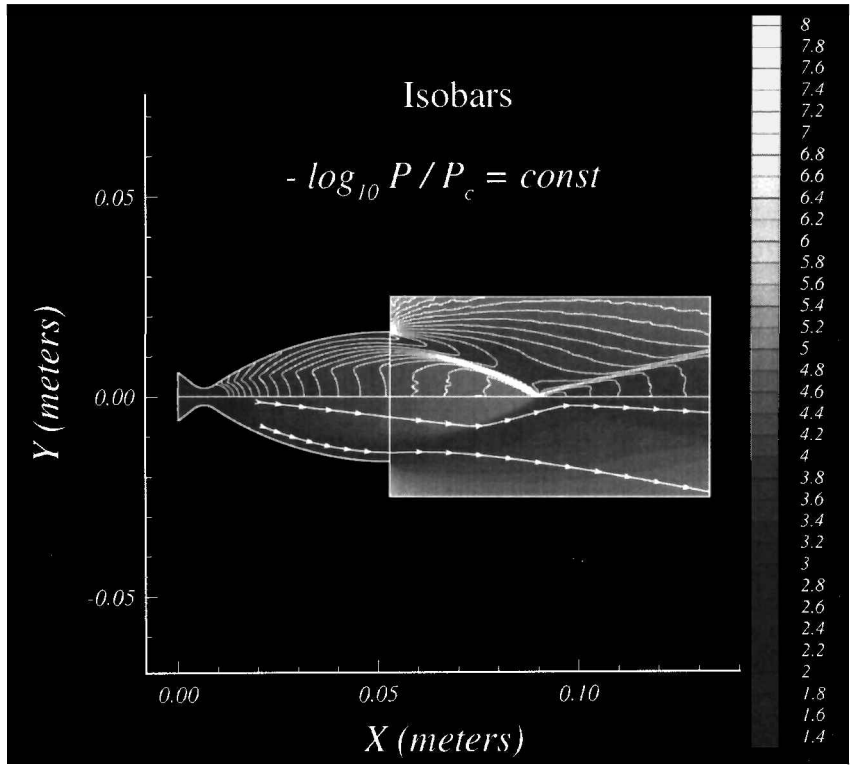

Fig. 8 Plume structure in the vicinity of the nozzle exit section.

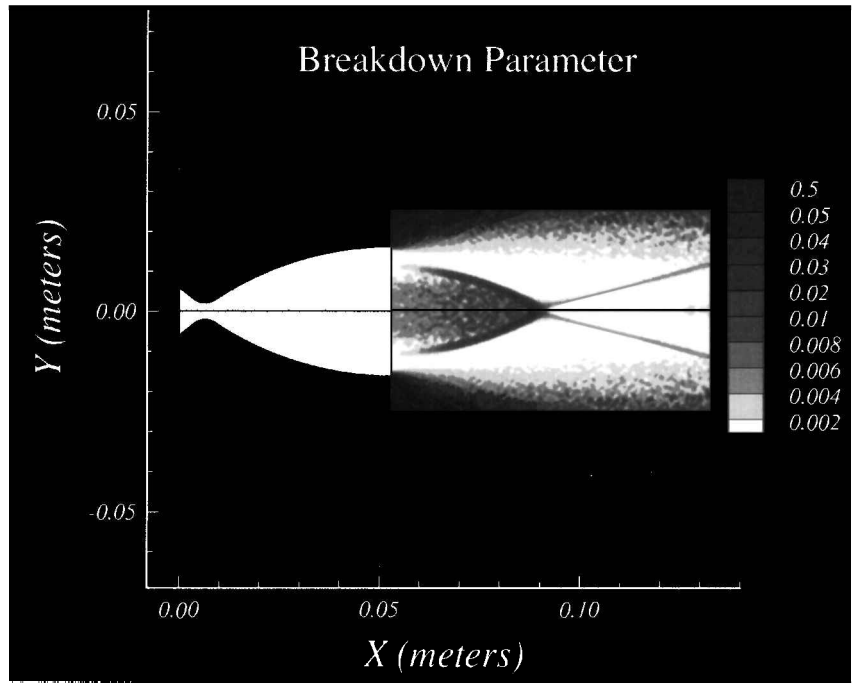

Fig. 9 Breakdown parameter map in the core of the plume.

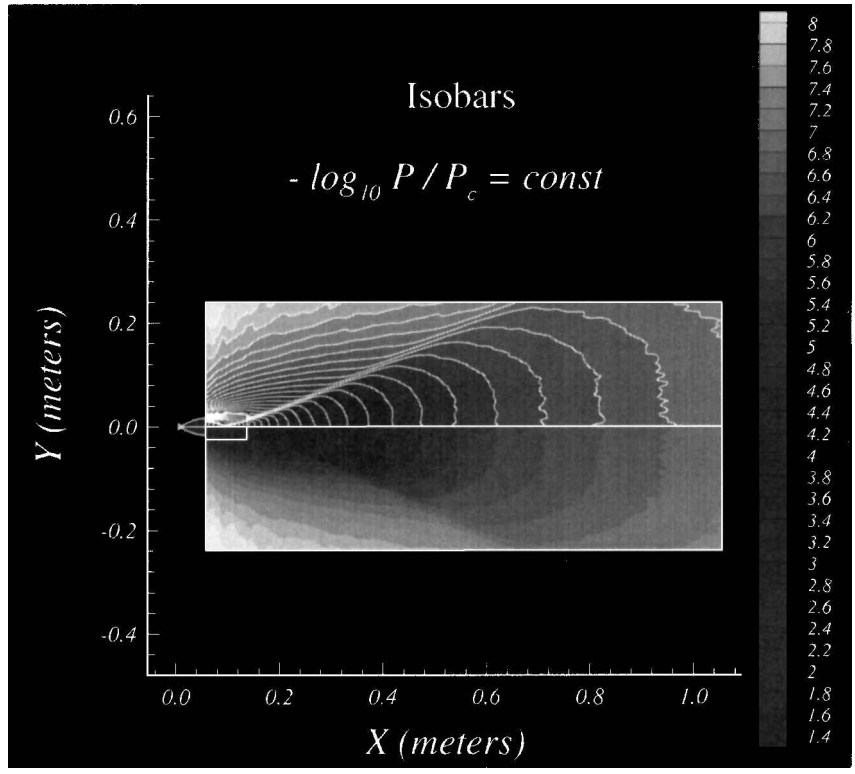

Fig. 10 Plume structure in the complete near field.

surfaces (Fig. 11) were then mounted on the satellite configuration with a tilt angle of 8 deg with respect to the diagonal plane, according to design specification. The simplified geometry of the XMM satellite consists of a squared base with a width of 3.124 m and a height of 1 m. The conical part is 6.48 m long. The flow conditions on the cylindrical surfaces constitute the input information for the TPMC simulation of the plume far field; this was carried out by assuming diffuse reflection with complete energy accommodation on the satellite surfaces. A typical three-dimensional view of the N_2 density distribution around the satellite is shown in Fig. 12. Some particles issued from the cylindrical surfaces do not interact with the satellite and leave undisturbed; other particles hit the satellite structure and are either reflected or absorbed. The interacting particles are responsible for the aerodynamic forces and moments on the satellite structure. Axial force distributions along the generatrices of the satellite conical part are shown in Figs. 13b and 13c. Figure 13b shows the species contributions, divided by corresponding molecular mass and molar fraction at the nozzle exit section (see Table 2), at a given circumferential angle. The distributions differ only slightly, and this indicates that the species are only weakly separated in the plume near and far fields. The upstream shift of the H_2 curve maximum is a consequence of the faster expansion of that light species

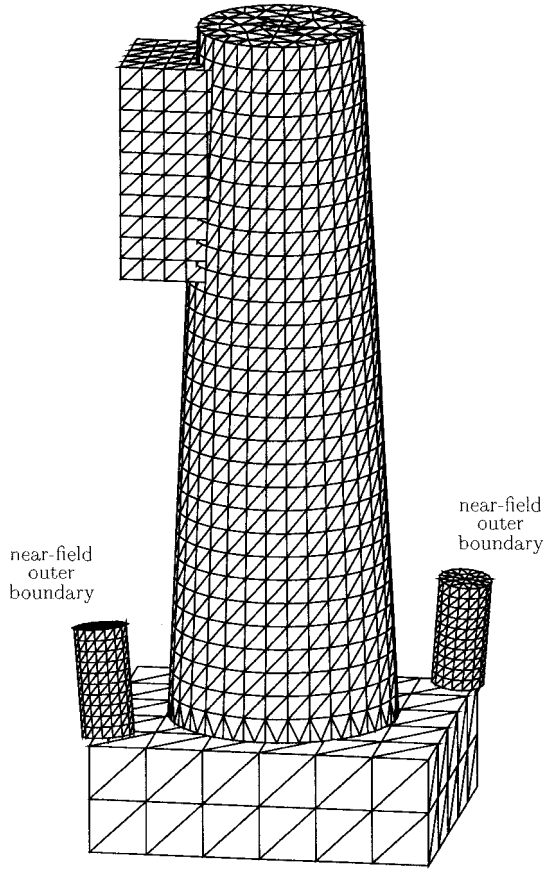

Fig. 11 Schematic configuration of the XMM satellite and cylindrical surfaces for the free-molecular calculation.

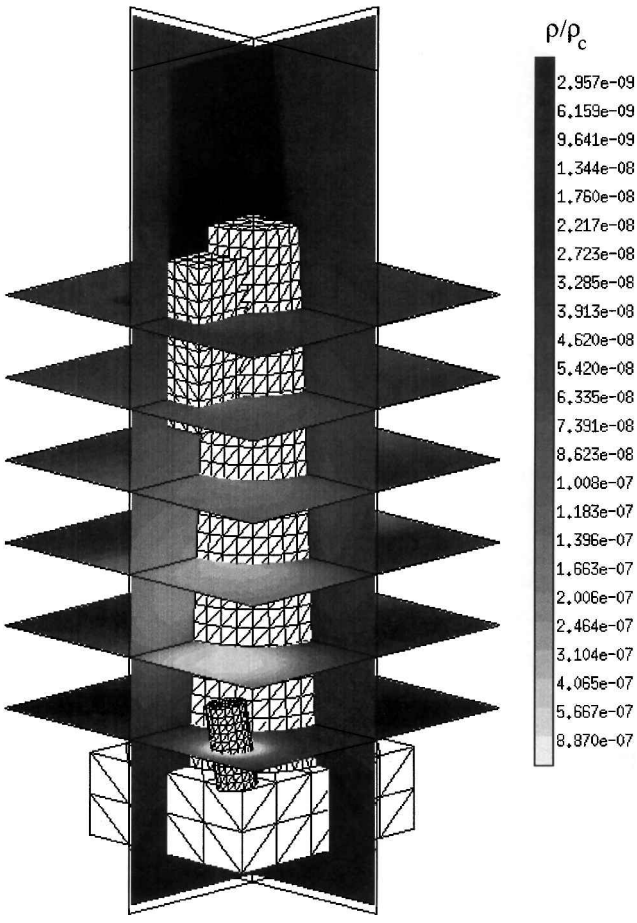

Fig. 12 N_2 density distribution around the satellite.

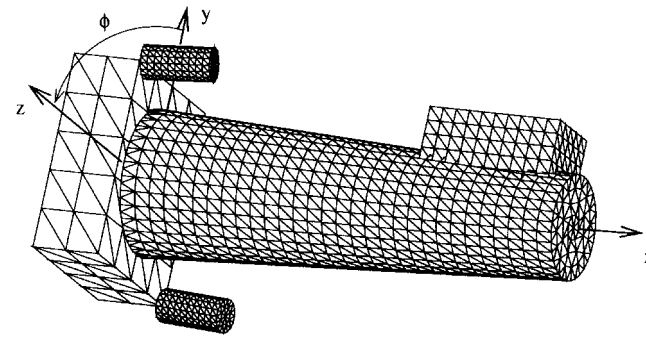

a) Coordinate system

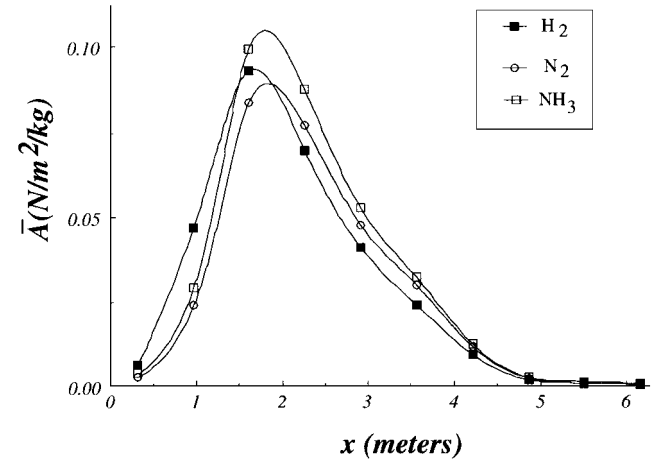

b) Species contributions at $\phi = 22.5$ deg

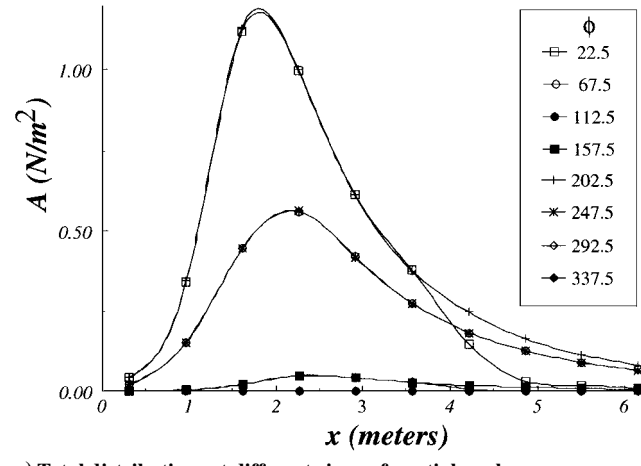

c) Total distributions at different circumferential angles

Fig. 13 Axial force distributions on the satellite conical body.

with respect to the others. Figure 13c shows the global axial-force distribution for different circumferential angles. All distributions show a peak between 2 and 3 m from the satellite base because of the specific behavior of the plume isobars (see Fig. 10). The corresponding total axial force amounts to 6.2 N, which represents 15.5% of the total nominal thrust ($2 \times 20 = 40$ N), clearly demonstrating the incompatibility between the 8-deg tilt angle of the thrusters and the 5% thrust-loss margin imposed by design considerations.

Conclusions

The application of the numerical multizone approach described in this work to a realistic design problem relative to the European Space Agency's XMM satellite led to the detection of a serious incompatibility between a preliminary design solution, i.e., orientation of the satellite thrusters, and the flight dynamics requirements imposed by the satellite mission. The awareness of such a conflict promoted a reevaluation of the feasibility of the higher-perigee injection maneuver for different tilt angles of the thrusters, with the

support of the associated plume impingement analysis. As a result of the tradeoff exercise (not performed by the authors), the optimum thruster tilt angle turned out to be 12 deg.

In conclusion, the application of the proposed methodology clearly shows that optimized satellite design can benefit from a complete numerical study of nozzle and plume flows as well as plume impingement. In this regard, the multizone approach on which the methodology is based appears to be very effective in providing detailed information about the whole flowfield to a degree of accuracy that cannot be achieved by approximate engineering methods for nozzle flows and analytical plume models.

Acknowledgments

We wish to acknowledge the courtesy of R. Brandt for supplying the 20-N hydrazine thruster data required for this study and D. Stramaccioni and A. Elfving for providing technical information relative to the X-Ray Multi-Mirror Mission satellite.

References

[1]Netterfield, M., "Validation of a Navier–Stokes Code for Thermochemical Nonequilibrium," AIAA Paper 92-2878, July 1992.

[2]Ivanov, M., and Markelov, G., "Efficient Algorithms of Statistical Simulation of Rarefied Flows on Parallel Computers," *Proceedings of the International Conference on the Methods of Aerophysical Research*, Vol. 3, Inst. for Theoretical and Applied Mechanics, Novosibirsk, Russia, 1997, pp. 103–108.

[3]Giordano, D., and Niccoli, R., "Analysis of the MSG Satellite Thruster and Plume Flows," *Proceedings of the 20th International Symposium on Rarefied Gas Dynamics*, Chinese Academy of Sciences, Beijing, PRC, 1997, pp. 519–524.

[4]Ivanov, M., Markelov, G., Kashkovsky, A., and Giordano, D., "Numerical Analysis of Thruster Plume Interaction Problems," *Proceedings of the Second European Spacecraft Propulsion Conference*, European Space Agency, Noordwijk, The Netherlands, 1997, pp. 603–610.

[5]Ivanov, M., Giordano, D., Markelov, G., and Marraffa, L., "Numerical Analysis of Back and Side Regions of Satellite Thruster Plumes," AIAA Paper 98-2470, June 1998.

[6]Ivanov, M., and Rogasinsky, S., "Theoretical Analysis of Traditional and Modern Schemes of the DSMC Method," *Proceedings of the 17th International Symposium on Rarefied Gas Dynamics*, VCH Verlagsgesellschaft, Weinheim, Germany, 1991, pp. 629–642.

[7]Bird, G., *Molecular Gas Dynamics and the Direct Simulation of Gas Flows*, Clarendon, Oxford, England, UK, 1994.

[8]Kogan, N., *Rarefied Gas Dynamics*, Plenum, New York, 1969.

[9]Woronowicz, M. S., and Rault, D. F. G., "On Plume Flowfield Analysis and Simulation Techniques," AIAA Paper 94-2048, June 1994.

[10]Gimelshein, S., Gorbachev, Y., Ivanov, M., and Kashkovsky, A., "Real Gas Effects on the Aerodynamics of 2D Concave Bodies in the Transitional Regime," *Proceedings of the 19th International Symposium on Rarefied Gas Dynamics*, Oxford Univ. Press, Oxford, England, UK, 1995, pp. 629–642.

[11]Ivanov, M., Markelov, G., Gimelshein, S., Mishina, L., Krylov, A., and Grechko, N., "Capsule Aerodynamics with Real Gas Effects from Free-Molecular to Near-Continuum Regimes," AIAA Paper 97-0476, Jan. 1997.

[12]Gimelshein, S., Ivanov, M., Markelov, G., and Gorbachev, Y., "Quasi-classical VRT Transitional Models in the DSMC Computations of Reacting Flows," *Proceedings of the 20th International Symposium on Rarefied Gas Dynamics*, Chinese Academy of Sciences, Beijing, PRC, 1997, pp. 711–716.

[13]Ivanov, M., Markelov, G., Gerasimov, Y., Krylov, A., Mishina, L., and Sokolov, E., "Free-Flight Experiment and Numerical Simulation for Cold Thruster Plume," AIAA Paper 98-0898, Jan. 1998.

[14]Ivanov, M., Kashkovsky, A., and Koppenwallner, G., "Results of Thruster Plume Interaction with Satellite," Hyperschall Technologie Göttingen, HTG-Rept. 96-1, Lindau, Germany, Jan. 1996.

[15]"BLT: A Computer Code for Solving the 2D/Axisymmetric Compressible Navier–Stokes Equations for Blunt Body Flows," AMTEC Engineering, Inc., AEI-T86100.03, Bellevue, WA, Aug. 1990.

R. G. Wilmoth
Associate Editor